# Molecular switches activated by electromagnetic pulses: First-principles calculations

Viviane Costa Felicíssimo,[*] Jonathan da Rocha Martins, Isabel Sager Boldt, and Helio Chacham[†]

*Departamento de Física, ICEx, Universidade Federal de Minas Gerais, Caixa Postal 702, 30123-970 Belo Horizonte, MG, Brazil*
(Received 19 February 2009; published 4 December 2009)

In the present work, we investigate, through *ab initio* molecular dynamics simulations, the molecular switching action (a hydrogen tautomerization reaction) in porphyrazine and phthalocyanine induced by electromagnetic pulses. We find that femtosecond pulses attainable from laser sources can induce the switching mechanism in porphyrazine and phthalocyanine through several reaction pathways. We investigate the dependence of the switching mechanism on the parameters (duration, frequency, and polarization) of the electromagnetic pulse and on isotopic substitutions. We also find that the dynamics of inner hydrogen switching in phthalocyanine can be induced by weaker electromagnetic pulses than in porphyrazine. This indicates that molecules of this class with larger numbers of aromatic rings will be more efficient in displaying the pulse-induced switching.

## I. INTRODUCTION

The progressive miniaturization of electronic devices required by the future generations of computers and other equipments has led to the emerging field of molecular electronics. An important component of a molecular electronic circuit is a molecular switch [1,2]. Molecular switches are specially designed single molecules that are able to alternate between at least two distinct and reversible states based on a change in molecular geometry through an external perturbation. Due to the potential technological applications, identifying and understanding molecular systems that are capable of switching behavior is attracting growing interest. Several experimental and theoretical investigations have focused on the possibility of realizing molecular switching induced and probed by scanning tunneling microscopy (STM) [3–7]. Recently, a molecular switch based on a molecule called naphthalocyanine has been demonstrated experimentally with low temperature STM [3]. The interconversion between the two switching states is related to the bistability of the position of the hydrogen atoms in the inner cavity of naphthalocyanine. Two related molecular systems that contain the same inner cavity as naphthalocyanine are the porphyrazine and phthalocyanine molecules, shown in Figs. 1(a) and 1(b), respectively. The figure also shows the inner hydrogen tautomerization reactions corresponding to the molecular switching processes.

In the last decades, the efficiency of using femtosecond laser pulses to guide and follow the nuclear motion, breaking or forming selected bonds during a chemical reaction has been demonstrated by experimental and theoretical studies [8–15]. In the present work, we investigate theoretically, through *ab initio* calculations, the possibility that strong infrared fields of few-cycle pulses can induce molecular switching in porphyrazine and phthalocyanine. We investigate the dependence of the switching mechanism on several parameters of the electromagnetic pulse and on possible isotopic substitutions. We find, in fact, that femtosecond pulses with intensities of $2.0 \times 10^{14}$ and $1.5 \times 10^{14}$ W/cm$^2$ can induce the switching mechanism in porphyrazine and phthalocyanine, respectively, through several reaction pathways. The strong laser fields that we predict to be necessary to induce molecular switching in porphyrazine and phthalocyanine would cause radiation damage to the molecules [16] and to device electrodes if these specific molecules were used in devices. Considering that fact, the main purpose of the present article is to provide a physical and chemical understanding of the reaction mechanisms that govern the dynamics of inner hydrogen transfer in porphyrazine and phthalocyanine. These two molecules can be considered as initial prototypes for larger molecular systems, belonging to the same class of molecules, which might present similar switching behavior under weaker fields.

## II. METHODOLOGY

### A. General

To describe the photo-induced dynamics, we employ a scheme based on *ab initio* molecular dynamics (MD) simulations, which has been used to predict, from first principles, structural, and dynamical properties of molecules and solids. In our theoretical treatment, the nuclear dynamics is de-
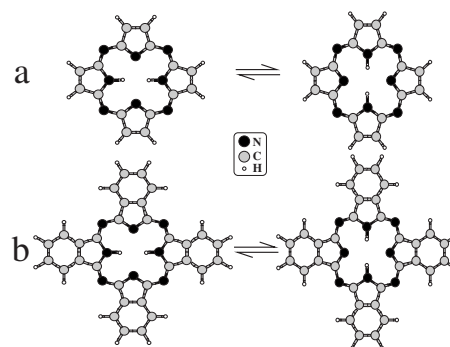


FIG. 1. Tautomerization reaction of (a) *trans*-porphyrazine and (b) *trans*-phthalocyanine.

*viviane@fisica.ufmg.br
†chacham@fisica.ufmg.br

scribed classically by the equation of motion based on forces derived from self-consistent density functional theory (DFT) [17] calculations, also including in the Hamiltonian an additional term corresponding to the interaction between an external laser field and the electrons and nuclei of the molecular system,

$$H = H_0 + V(t). \qquad (1)$$

Here, $H_0$ is the time-independent electronic Hamiltonian and $V(t)$ contains the interaction between the molecule and the time-dependent laser field $\mathbf{E}(t)$ in accordance with the expression

$$V(t) = -\mathbf{E}(t) \cdot \left[ \sum_I Z_I \mathbf{R}_I - \sum_i \mathbf{r}_i \right]. \qquad (2)$$

In Eq. (2), $Z_I$ is the atomic number of the $I$th nucleus and $\mathbf{R}_I$ and $\mathbf{r}_i$ are the coordinates of the $I$th nucleus and $i$th electron, respectively. The electric field $\mathbf{E}(t)$ of the electromagnetic radiation is given by

$$\mathbf{E}(t) = \mathbf{e}\sqrt{\frac{2I(t)}{c\varepsilon_0}}\cos[\omega(t-t_0)+\varphi], \qquad (3)$$

where $\mathbf{e}$ is the polarization vector of the light, $c$ is the speed of light, $\varepsilon_0$ is the permittivity, and $I(t)$ describes the temporal shape of the laser pulse, which is modulated in the calculations by a Gaussian

$$I(t) = I_0 \exp\left[ -\ln 2\left(\frac{t-t_0}{\tau}\right)^2 \right]. \qquad (4)$$

Here, $I_0$ is the peak intensity of radiation, $\tau$ is the half width at half maximum (HWHM), interpreted as the laser pulse duration, and $t_0$ is the peak position of the laser pulse.

### B. DFT and computational aspects

All calculations and simulations have been performed on the framework of Kohn-Sham density functional theory [17] within the generalized gradient approximation (GGA) [18] and norm-conserving pseudopotentials [19] as implemented in the SIESTA program [20]. We modified the SIESTA program to include the temporal dependence of the external electric field as given by Eq. (3). The solutions of the Kohn-Sham equations are expanded as a linear combination of atomic orbitals (LCAO) of finite range. We use a double-zeta basis set plus polarization orbitals. The *ab initio* level of the MD method is crucial in our simulation due to the large sensitivity of the nuclear dynamics to the electronic polarization by the laser field. In the molecular dynamics simulations, the Verlet algorithm has been used for integrating the equations of motions for each time step of 0.2 fs during a time interval of 3 ps. The initial temperature of the molecular dynamics simulations is 300 K.

### C. Shape and parameters of the laser pulse

The femtosecond laser pulse is modulated by a Gaussian function centered at the time $t_0 = 0$ fs. In all simulations, the ir field is assumed to be nearly in resonance with the N-H
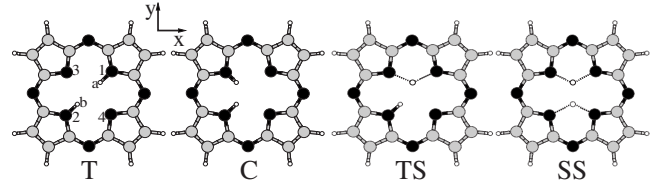


FIG. 2. The four relevant structures to describe the inner hydrogen atoms transfer in porphyrazine: trans-porphyrazine (T), *cis*-porphyrazine (C), *trans-cis* transition state (TS), and second-order saddle point (SS).

stretching vibrational frequencies, $\omega \approx \omega_{NH}$. The phase $\varphi = 0$ has been used to obtain the maximum intensity of the few-cycle ir pulse at the instant $t_0 = 0$ fs.

The laser pulse used to induce the inner hydrogen transfer in *trans*-porphyrazine has been modulated with the following parameters: duration $\tau = 10$ fs, intensity $I_0 = 2.0 \times 10^{14}$ W/cm$^2$, and frequency $\omega = 0.45$ eV (in units of $\hbar\omega$, which we will use henceforth). The intensity $I_0 = 2.0 \times 10^{14}$ W/cm$^2$ corresponds to the electric field strength of 3.88 V/Å. In order to study the dependence of the switching mechanism of the inner hydrogen atoms in trans-porphyrazine, the frequency, and duration of the laser pulse are alternatively changed to $\omega = 0.42$ eV and $\tau = 15$ fs, respectively. We consider different cases with distinct initial orientation of the molecular system relative to the polarization vector ($\mathbf{e}$) of the electromagnetic radiation. In one case, the polarization vector of the electromagnetic radiation is parallel ($\mathbf{E}_\parallel$) to the axis along the N-H$\cdots$H-N in *trans*-porphyrazine. In the other case, there is an angle of 45° between the polarization vector of the electromagnetic radiation ($\mathbf{E}_\angle$) and the axis along the N-H$\cdots$H-N in *trans*-porphyrazine. In the case of *trans*-phthalocyanine, the light-induced molecular dynamics has been studied with the following pulse parameters: duration $\tau = 15$ fs, intensity $I_0 = 1.5 \times 10^{14}$ W/cm$^2$, and frequency $\omega = 0.45$ eV, with the nonparallel orientation ($\mathbf{E}_\angle$) of the molecular system relative to the polarization vector of the electromagnetic field, as described above.

## III. RESULTS

### A. Porphyrazine molecule

#### 1. Potential energy surface

Before we present the results of our molecular dynamics simulations of porphyrazine, let us describe its potential energy surface and the possible reaction pathways for inner hydrogen tautomerization [21]. The equilibrium structure of free-base porphyrazine exhibits the *trans* form [see Fig. 1(a)]. A set of four structures—*trans*-porphyrazine (T), *cis*-porphyrazine (C), *trans-cis* transition state (TS), and second-order saddle point (SS)—which are presented in Fig. 2, are relevant to study the dynamics of inner hydrogen tautomerization in *trans*-porphyrazine [Fig. 1(a)] [21]. In Fig. 2, the hydrogen and nitrogen atoms in the inner cavity of *trans*-porphyrazine are named as $H_a$, $H_b$, $N_1$, $N_2$, $N_3$, and $N_4$.

The potential energy surface (PES) that provides the relative energies of the structures T, C, TS, and SS is presented
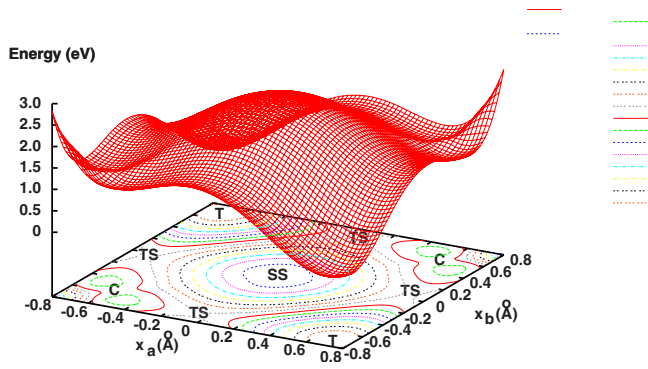
FIG. 3. (Color online) Potential energy surface of porphyrazine showing the *trans* (T) minimum, the metastable *cis* (C) minimum, the *trans-cis* transition state (TS), and the second-order saddle point (SS). The spatial coordinates $x_a$ and $x_b$ are, respectively, the $x$ component of hydrogen a and b of *trans*-porphyrazine (T) as shown in Fig. 2.



FIG. 4. (Color online) Potential energy curves of porphyrazine along $x_b$ when $x_a = -x_b$ (solid line) and $x_a = 0.7$ Å (dashed line). The spatial coordinates $x_a$ and $x_b$ are described in Fig. 3.

in Fig. 3. The PES is calculated as a function of the Cartesian coordinates $x_a$ and $x_b$, which are defined as the $x$ component of the two inner hydrogen atoms $H_a$ and $H_b$ of porphyrazine, respectively, when the origin of the Cartesian system is located at the center of the molecule (see T structure of Fig. 2). The PES of Fig. 3 shows two global minima that are attributed to the two tautomers of *trans*-porphyrazine presented in Fig. 1(a). Other two metastable minima represent the two tautomers of *cis*-porphyrazine. The transition state is shown in Fig. 3 as being the structure that connects the *trans*-porphyrazine to *cis*-porphyrazine, while the second-order saddle point is the transitory specie that converts *trans*- to *trans*-porphyrazine or *cis*- to *cis*-porphyrazine.

The analysis of Fig. 3 allows us to suggest two distinct mechanisms to describe the dynamics of inner hydrogen transfer in *trans*-porphyrazine [Fig. 1(a)]. In the first one, the switching of the inner hydrogen atoms in *trans*-porphyrazine occurs simultaneously following the reaction pathway T→SS→T. It characterizes a single step reaction which occurs through the second-order saddle point. By contrast, in the second mechanism, the successive hydrogen transfer happens via the reaction pathway T→TS→C→TS→T. It occurs in two steps and involves the participation of two transition states (TS) and the formation of the intermediate state C (the metastable state *cis*-porphyrazine).

The relative energies of T, C, TS, and SS structures in the two reaction pathways discussed above are clearly seen in Fig. 4, where cuts on the PES along $x_b$ are shown for the cases where $x_a = -x_b$ (solid line) and $x_a = 0.7$ Å (dashed line). The solid line shows the variation in the potential energy along the reaction pathway T→SS→T, while the dashed line represents the conversion from *trans*-porphyrazine to *cis*-porphyrazine. It is observed that while the interconversion T→SS→T has an activation barrier of 2.65 eV, the alternative reaction pathway via the intermediate state *cis*-porphyrazine shows for the first step reaction, T→TS→C, a smaller barrier of 1.51 eV.

### 2. Molecular dynamics simulations

The main objective of this work is to investigate, through molecular mechanics, if the control of the dynamics of $H_a$
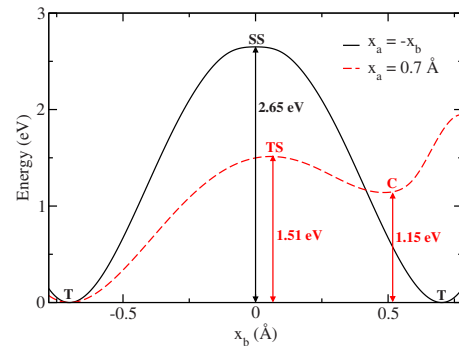
and $H_b$ following different reaction mechanisms such as simultaneous switching (T→SS→T) or successive transfer (T→TS→C→TS→T) can be done using femtosecond laser pulses. The proper choice of the parameters of the pulse guides the reaction, for example, in one or other pathway. In this section, we will consider several possible variations in the parameters of the laser pulse such as frequency, duration, and polarization, and investigate the effect of those parameters on the dynamics of the inner hydrogen transfer. In addition, we will study how the switching mechanism depends on the isotopic substitution in prophyrazine.

In order to analyze the temporal sequence of the nuclear dynamics induced by the femtosecond laser pulse, and relate that to the molecular switching states shown in Fig. 1, we propose a geometrical order parameter $d$, which is a function of the atomic coordinates of the molecule. This order parameter assumes extreme values $+1$ and $-1$ when the molecule is, respectively, at the left and right structural configurations in Fig. 1. The parameter is defined by the equation

$$d = \frac{|d_{1a} - d_{2a}| - |d_{3a} - d_{4a}| + |d_{1b} - d_{2b}| - |d_{3b} - d_{4b}|}{2|d_{1a}^{eq} - d_{2a}^{eq}|}, \quad (5)$$

where $|d_{1a}^{eq} - d_{2a}^{eq}| = 1.996$ Å.

In Eq. (5), the indexes 1, 2, 3, and 4 make reference to the numeration given to the nitrogen atoms of *trans*-prophyrazine in Fig. 2, while $a$ and $b$ are the indexes of the hydrogen atoms in the inner cavity of porphyrazine. Therefore, $d_{ij}$ is the distance, in Å, from the $i$-th nitrogen atom to the $j$-th hydrogen atom in porphyrazine. The quantity $|d_{1a}^{eq} - d_{2a}^{eq}|$ is a normalization factor written as the module of the difference between the equilibrium distances of $d_{1a}$ and $d_{2a}$, at the initial time of the dynamics. From Eq. (5), it is possible to conclude that the $d$ parameter assumes values close to $+1$ or $-1$ when the *trans*-porphyrazine is formed. The signal exchange of $d$ function from $+1$ to $-1$ describes the switching of $H_a$ and $H_b$ from $N_1$ and $N_2$ to $N_3$ and $N_4$, respectively. When $d$ is close to zero, this indicates the formation of the *cis*-porphyrazine.

The temporal dependence of the geometrical order parameter $d$ was investigated for several molecular dynamics simulations, each one with a different set of electromagnetic pulse parameters. These temporal dependences $d(t)$ are shown in
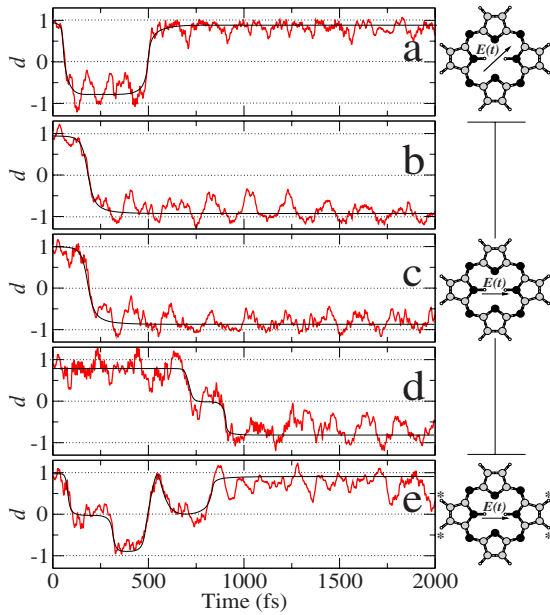
FIG. 6. Light-induced molecular dynamics of *trans*-porphyrazine. The polarization vector of the light is parallel ($\mathbf{E}_\parallel$) to the N-H⋯H-N axis of *trans*-porphyrazine. The parameters of the laser pulse are: $\tau=10$ fs, $\omega=0.45$ eV, and $I_0=2.0\times10^{14}$ W/cm$^2$.



FIG. 5. (Color online) Time dependence of the geometrical parameter $d$ given by Eq. (5) for the dynamics of *trans*-porphyrazine induced by distinct light pulses: (a) $\tau=15$ fs, $\omega=0.45$ eV, and $\mathbf{E}_\perp$, (b) $\tau=15$ fs, $\omega=0.45$ eV, and $\mathbf{E}_\parallel$, (c) $\tau=10$ fs, $\omega=0.45$ eV, and $\mathbf{E}_\parallel$, (d) $\tau=10$ fs, $\omega=0.42$ eV, and $\mathbf{E}_\parallel$, and (e) $\tau=10$ fs, $\omega=0.42$ eV, and $\mathbf{E}_\parallel$. In panel (e), the hydrogen atoms are replaced by deuterium. The (c) panel corresponds to the dynamics shown in Fig. 6. The dark lines represent a qualitative average of the $d$ parameter in function of the time.

Fig. 5. A qualitative average behavior $d$ that excludes short-term oscillations is also shown in this figure as a guide to the eye. In Fig. 5, we consider several variations in the pulse parameters: from (b) to (c), the pulse duration $\tau$ is reduced by 1/3; from (c) to (d), the pulse frequency $\omega$ is reduced by 6.6%; from (b) to (a), the polarization vector of the electromagnetic field changes from being parallel to the N-H⋯H-N axis of *trans*-porphyrazine ($\mathbf{E}_\parallel$) to a nonparallel orientation ($\mathbf{E}_\perp$), forming an angle of 45° with that axis; finally, from (d) to (e), the external hydrogen atoms indicated in the figure by asterisks are replaced by deuterium atoms. In the following, we will analyze the effect of each variation.

Let us start by discussing the result presented in Fig. 5(c). In this case, the parameters of the laser pulse are $\tau=10$ fs, $\omega=0.45$ eV, and $I_0=2.0\times10^{14}$ W/cm$^2$. Analyzing the temporal dependence of $d(t)$ function, we observe the following behavior: $d(t)\approx1$ for $t<188$ fs, $d(t)=0$ for $t=188$ fs, and $d(t)\approx-1$ for $t>188$ fs. This means that the dynamics starts from *trans*-porphyrazine and, at the time $t=188$ fs, the two inner hydrogen atoms of porphyrazine are transferred originating the switched *trans*-porphyrazine from $t\approx222$ fs. This behavior shows that the hydrogen atoms $H_a$ and $H_b$ are simultaneously transferred following the reaction pathway T→SS→T, where the SS structure is formed at the time $t=188$ fs, see Fig. 6. The tautomerization reaction is finalized at the time $t\approx222$ fs. This dynamics is followed during a time interval of $t\approx3$ ps and the switched *trans*-porphyrazine keeps its structure stable up to the final time of the dynamics. We have also performed a simulation similar
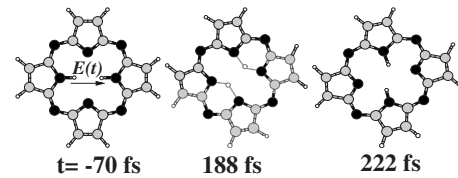
to the one presented in Fig. 5(c), but with the phase $\varphi$ [see Eq. (3)] changed from zero to $\pi/2$. The resulting dynamics is almost indistinguishable from the one of Fig. 5(c), indicating a negligible dependence of the pulse phase on the hydrogen transfer dynamics.

Changing the pulse duration: from Figs. 5(c), we increase the duration of the laser pulse from $\tau=10$ fs to $\tau=15$ fs. The result show a rather similar qualitative and quantitative behavior. This means that the dynamics of inner hydrogen transfer in *trans*-porphyrazine has not been sensitive to such a change in the duration of the laser pulse.

Changing the pulse polarization: a strong effect is observed when we change the orientation of the molecule relative to the polarization vector of the electromagnetic field. This is presented in Figs. 5(b) and 5(a) for parallel ($\mathbf{E}_\parallel$) and nonparallel ($\mathbf{E}_\perp$) orientations of the laser pulse polarization, respectively. In Fig. 5(a), the hydrogen transfer dynamics follows the reaction mechanism T→SS→T, where the SS structure is formed earlier (at $t=65$ fs) than in Fig. 5(b). At $t=495$ fs, the inner hydrogen atoms in porphyrazine follow a new simultaneous transfer returning to its initial structure. The earlier dynamics in Fig. 5(a) might be due to the fact that the electric field is oriented along the same direction of hydrogen transfer. That is, the electric field is oriented in such a way that it excites the most the normal vibrational modes that are approximately in the direction of the saddle point for hydrogen transfer.

Changing the pulse frequency: a comparison between the curves of panels (c) and (d), where the frequency of the electromagnetic field is changed from 0.45 to 0.42 eV, shows that the dynamics of inner hydrogen transfer in *trans*-porphyrazine is very sensitive to the frequency of the electromagnetic field. Two main effects result from the pulse frequency reduction. First, the system remains much longer in the initial $d\approx+1$ initial state. Second, the transition from $d\approx+1$ to $d\approx-1$ now involves a period of time (of about 200 fs) where the systems stays with $d\approx0$. Therefore, different from the previous (a), (b), and (c) cases (all corresponding to $\omega=0.45$ eV), in case (d) (with reduced frequency) the hydrogen atoms $H_a$ and $H_b$ follow a dynamics of successive transfer in two steps, via the reaction pathway T→TS→C →TS→T, where the transition state TS of the first step is formed at $t\approx700$ fs, leading to the formation of the intermediate state C. At $t\approx900$ fs, the second transition state TS is formed which results in the transfer of the second hydrogen atom which leads to the formation of the structure T.

Naively, one might expect that the hydrogen transfer dynamics in the two-step reaction pathway T→TS→C→TS

→T, observed in panel (d), would occur more often because it has a smaller activation energy (1.51 eV) than the single step reaction T→SS→T, which has a higher activation energy of 2.65 eV (see Fig. 4). However, we find the opposite: among the four dynamics considered so far, only the one with reduced frequency follows the low-activation-energy pathway. We suggest that the higher frequency laser field is nearly resonant with vibrational modes that have a large component of N-H stretching of porphyrazine and, due to this, a significant part of the energy that the molecule absorbs from the light becomes localized on the N–H bonds, and the tautomerization reaction is faster in this case. On the other hand, when $\omega = 0.42$ eV, the laser frequency would be less in resonance with the N-H stretching related modes and, therefore, other vibrational modes such as C-H stretching, for example, would also be excited. The reaction would therefore occur at a later time, and through a pathway that has a smaller barrier.

The effect of isotopic substitutions: in Fig. 5(e) we show a molecular dynamics simulation with the same light pulse parameters as in Fig. 5(d). However, in this case, four hydrogen atoms, indicated by asterisks in Fig. 5(e), are replaced by deuterium atoms. From the time dependence of the $d$ parameter in Fig. 5(e), we observe an earlier and more complicated inner hydrogen transfer dynamics in porphyrazine than the one shown in panel (d). The $d(t)$ curve in panel (e) follows a dynamics which might be described by a five-step reaction mechanism T→TS→C→TS→T→SS→T→TS→C→TS→T. The first transition state TS is formed at the time $t = 88$ fs, which is 600 fs earlier than the equivalent transition state formed in panel (d). The isotopic substitution makes the C-D stretching modes to be out of resonance with the light frequency. We suggest that the absorbed energy from the light becomes more localized on the N–H bonds, resulting in an earlier dynamics than the one presented in Fig. 5(d). The isotopic substitution could therefore be used as a tool to localize the absorbed energy from the light at specific regions of the molecular system.

### 3. Molecular properties during the light pulse interaction

We have described so far the time dependence of the geometrical order parameter $d$, and the inner hydrogen tautomerization reaction of porphyrazine, due to different electromagnetic pulses. Notice, however, that the earliest modification in $d(t)$ in Fig. 5 starts well after the action of the light pulse (which has a time duration on the order of $\tau \approx 10–15$ fs) ends. Therefore, the role of the light pulse is to provide initial kinetic energy to the atoms of the molecule, which will later lead to the tautomerization reaction. Let us now investigate how the light pulse changes the properties of the molecule during its action. This might give us information on the action mechanism of the light pulse.

In Fig. 7, we show the time dependence of three molecular properties of *trans*-porphyrazine [the total energy, the induced dipole moment and the Highest Occupied Molecular Orbital (HOMO)—Lowest Unoccupied Molecular Orbital (LUMO) energy gap] simultaneously with the temporal dependence of the electric field of the pulse, which in this case has the parameters $\tau = 10$ fs, $\omega = 0.45$ eV, and $I_0 = 2.0$
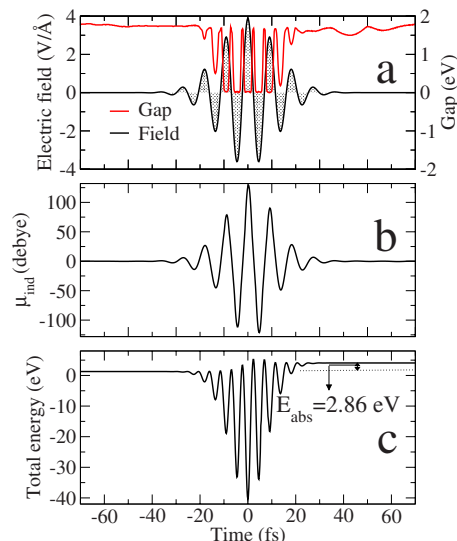


FIG. 7. (Color online) Time dependence of the electric field $\mathbf{E}(t)$ [Eq. (3)] (a) for the dynamics of *trans*-porphyrazine shown in Fig. 6. The parameters of the laser pulse are: $\tau = 10$ fs, $\omega = 0.45$ eV, and $I_0 = 2.0 \times 10^{14}$ W/cm$^2$. Panel (a) shows also the time dependence of the HOMO-LUMO gap. Panels (b) and (c) show the time dependence of the induced dipole moment ($\mu_{ind}$) and the total energy of the molecule, respectively.

$\times 10^{14}$ W/cm$^2$. This is the pulse that leads to the dynamics of inner hydrogen transfer in *trans*-porphyrazine presented in Figs. 5(c) and 6.

The panel (a) in Fig. 7 shows that the pulsed electric field reduces the HOMO-LUMO gap of porphyrazine. This gap even goes to zero when the intensity of the electric fields exceeds 2 V/Å. This reduction in the gap energy is caused by the terms $\mathbf{E}(t) \cdot \mathbf{r}_i$ in Eq. (2), which cause a significant potential perturbation on the electronic states and eigenvalues. Similar gap reductions due to strong electric fields have also been predicted for defective carbon nanotubes [22]. The modifications of the electronic states and eigenvalues originated from the large electric field also distort the molecular electronic density, polarizing the molecule and creating large induced dipole moments ($\mu_{ind}$). The time dependence of $\mu_{ind}$ follows the temporal oscillation of the electric field, as one can see in Fig. 7(b). The interaction of the molecular system with the laser pulse allows the molecule to absorb energy. The time dependence of the total energy of the molecule is shown in Fig. 7(c). The total energy oscillates during the time interval of molecular interaction with the light and it becomes constant after the end of the pulse. Panel (c) of Fig. 7 shows a net increase in energy of 2.86 eV after the electromagnetic pulse ends. This absorbed energy allows *trans*-porphyrazine to follow the dynamics via the one step reaction pathway T→SS→T presented in Figs. 5(c) and 6. The amount of energy absorbed in this is enough to overcome the activation energy of 2.65 eV (see Fig. 4). At this point, we would like to pay attention to the fact that the absorbed energy is not the only determinant factor on the inner hydrogen switching dynamics. To demonstrate that, we performed simulations similar to that of Fig. 5(c) but with the following parameters for the duration and intensity of the laser pulse:
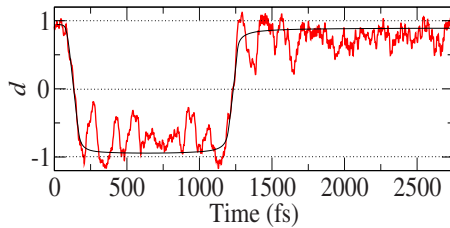
FIG. 8. (Color online) Time dependence of the geometrical parameter $d$ given by Eq. (5) for the dynamics of *trans*-phthalocyanine induced by distinct a light pulse with the following characteristics: $\tau=15$ fs, $\omega=0.45$ eV, and $I_0=1.5\times10^{14}$ W/cm$^2$. The polarization vector of the light is nonparallel ($\mathbf{E}_\angle$) to the N-H$\cdots$H-N axis of *trans*-phthalocyanine. The dark line represent a qualitative average of the $d$ parameter in function of the time.

(i) $\tau=5$ fs and $I_0=2.03\times10^{14}$ W/cm$^2$; (ii) $\tau=20$ fs and $I_0=1.8\times10^{14}$ W/cm$^2$. In both cases, the duration of the pulse was changed but the pulse intensity was adjusted so as to result in a value of the absorbed energy that is similar to the one of the original simulation (2.86 eV). In simulations (i) and (ii), we do not observe the dynamics of inner hydrogen transfer in *trans*-porphyrazine. The molecule just vibrates around the initial equilibrium geometry. These results demonstrate the importance of using a controlled set of the laser field parameters to induce a desired dynamics in the molecule.

### B. Phthalocyanine molecule

In the same way as it has been done for the porphyrazine molecule, the temporal evolution of the inner hydrogen transfer dynamics of *trans*-phthalocyanine was also monitored through the analysis of the temporal dependence of the geometrical order parameter $d$ given by Eq. (5). For the phthalocyanine molecule the normalization factor $|d_{1a}^{eq}-d_{2a}^{eq}|$ is equal to 2.019 Å. The temporal dependence of the geometrical order parameter $d(t)$ is shown in Fig. 8 for an electromagnetic pulse with the following parameters: $\tau=15$ fs, $I_0=1.5\times10^{14}$ W/cm$^2$, and $\omega=0.45$ eV. The polarization vector of the light is nonparallel ($\mathbf{E}_\angle$) to the N-H$\cdots$H-N axis of *trans*-phthalocyanine, forming an angle of 45° with this axis. The qualitative average behavior of the $d(t)$ parameter is shown in Fig. 8 by a dark line. Figure 8 shows that, upon the excitation by the light pulse, $d(t)$ changes from $\approx1$ to $\approx-1$ at $t\approx140$ fs, and back to $d(t)\approx1$ at $t\approx1230$ fs, and phthalocyanine follows the reaction path T$\rightarrow$SS$\rightarrow$T$\rightarrow$SS$\rightarrow$T.

Let us compare the simulation shown in Fig. 8 for the phthalocyanine molecule with the similar one, shown in Fig. 5(a), performed for the porphyrazine molecule. The only difference between the pulse parameters used in those simulations is the intensity of the electric field. The field intensities were chosen to be close to a minimum threshold value to produce the inner hydrogen tautomerization reaction. We ob-

serve that the inner hydrogen switching in phthalocyanine occurs for a pulse intensity of $I_0=1.5\times10^{14}$ W/cm$^2$, which is smaller than the intensity $I_0=2.0\times10^{14}$ W/cm$^2$ that is necessary to induce the inner hydrogen transfer in porphyrazine.

We propose that the reduction in the minimum intensity to cause inner hydrogen switching in phthalocyanine, as compared porphyrazine, is due to the introduction of additional aromatic rings that make the electronic density of the molecule more polarizable. This is consistent with the calculated induced dipole moments of phthalocyanine ($\mu_{\mathrm{ind}}=242.89$ debye) and porphyrazine ($\mu_{\mathrm{ind}}=86.55$ debye) upon a light intensity of $1.5\times10^{14}$ W/cm$^2$ and for the nonparallel polarization of the electric field ($\mathbf{E}_\angle$). The induced dipole moment calculated for phthalocyanine is about 2.8 times larger than the one for porphyrazine upon the application of the same electric field. Due to its more polarizable electronic density, the phthalocyanine molecule absorbs more energy from the electromagnetic pulse in the situation shown in Fig. 8 ($E_{\mathrm{abs}}=3.13$ eV) than porphyrazine does in the situation shown in Fig. 5(a) ($E_{\mathrm{abs}}=2.24$ eV), even though the pulse intensity is lower for phthalocyanine. For this reason, the dynamics of inner hydrogen switching in phthalocyanine can be induced by weaker electromagnetic pulses than in porphyrazine. This suggests that molecules of the class of porphyrazine with larger numbers of aromatic rings will be more efficient in displaying the pulse-induced tautomerization reaction. We should stress out that a quantitative description of this molecular-size effect might demand the use of exact-exchange functionals.

### IV. SUMMARY

In summary, we presented quantum molecular dynamics simulations to investigate the dynamics of inner hydrogen transfer (molecular switching) in *trans*-prophyrazine and *trans*-phthalocyanine induced and controlled by femtosecond laser pulses. We investigated the dependence of the switching mechanism on the parameters (duration, frequency, and polarization) of the electromagnetic pulse. We also investigated the effect of isotopic substitution on the molecular switching dynamics of porphyrazine. We also find that the dynamics of inner hydrogen switching in phthalocyanine can be induced by weaker electromagnetic pulses than in porphyrazine. This suggests that molecules of the class of porphyrazine with larger numbers of aromatic rings will be more efficient in displaying the pulse-induced tautomerization reaction.

### ACKNOWLEDGMENTS

[1] C. Joachim, J. K. Gimzewski, and A. Aviram, Nature (London) **408**, 541 (2000).

[2] P. M. Mendes, A. H. Flood, and J. F. Stoddart, Appl. Phys. A: Mater. Sci. Process. **80**, 1197 (2005).

[3] P. Liljeroth, J. Repp, and G. Meyer, Science **317**, 1203 (2007).

[4] L. Grill, J. Phys.: Condens. Matter **20**, 053001 (2008).

[5] F. Moresco, G. Meyer, K. H. Rieder, H. Tang, A. Gourdon, and C. Joachim, Phys. Rev. Lett. **86**, 672 (2001).

[6] V. Iancu and S. W. Hla, Proc. Natl. Acad. Sci. U.S.A. **103**, 13718 (2006).

[7] E. G. Emberly and G. Kirczenow, Phys. Rev. Lett. **91**, 188301 (2003).

[8] A. H. Zewail, J. Phys. Chem. A **104**, 5660 (2000).

[9] V. C. Felicíssimo, F. F. Guimarães, F. Gel'mukhanov, A. Cesar, and H. Ågren, J. Chem. Phys. **122**, 094319 (2005).

[10] T. Dumitrică, M. E. Garcia, H. O. Jeschke, and B. I. Yakobson, Phys. Rev. Lett. **92**, 117401 (2004).

[11] A. H. Romero, M. E. Garcia, F. Valencia, H. Terrones, M. Terrones, and H. O. Jeschke, Nano Lett. **5**, 1361 (2005).

[12] D. Geppert, L. Seyfarth, and R. de Vivie-Riedle, Appl. Phys. B: Lasers Opt. **79**, 987 (2004).

[13] R. de Vivie-Riedle and U. Troppmann, Chem. Rev. (Washington, D.C.) **107**, 5082 (2007).

[14] H. Tamura, S. Nanbu, T. Ishida, and H. Nakamura, J. Chem. Phys. **125**, 034307 (2006).

[15] M. Ndong, L. Bomble, D. Sugny, Y. Justum, and M. Desouter-Lecomte, Phys. Rev. A **76**, 043424 (2007).

[16] L. V. Keldysh, Sov. Phys. JETP **20**, 1307 (1965).

[17] R. G. Parr and W. Yang, *Density-Functional Theory of Atoms and Molecules* (Oxford University Press, New York, 1989).

[18] J. P. Perdew, K. Burke, and M. Ernzerhof, Phys. Rev. Lett. **77**, 3865 (1996).

[19] N. Troullier and J. L. Martins, Phys. Rev. B **43**, 1993 (1991).

[20] J. M. Soler, E. Artacho, J. D. Gale, A. García, J. Junquera, P. Ordejón, and D. Sánchez-Portal, J. Phys.: Condens. Matter **14**, 2745 (2002).

[21] Y. Z. Huang and S. Y. Ma, J. Mol. Struct.: THEOCHEM **684**, 217 (2004).

[22] S. S. Alexandre, M. S. C. Mazzoni, and H. Chacham, Phys. Rev. Lett. **100**, 146801 (2008).